Biomaterials 34 (2013) 4810–4817

Contents lists available at SciVerse ScienceDirect

Biomaterials

journal homepage: www.elsevier.com/locate/biomaterials

Self-assembled, functionalized graphene and DNA as a universal platform for colorimetric assays

Yu Tao, Youhui Lin, Jinsong Ren*, Xiaogang Qu*

State Key Laboratory of Rare Earth Resources Utilization and Laboratory of Chemical Biology, Changchun Institute of Applied Chemistry, Graduate School of the Chinese Academy of Sciences, Chinese Academy of Sciences, Changchun, Jilin 130022, China

ARTICLE INFO

Article history:
Received 4 February 2013
Accepted 14 March 2013
Available online 30 March 2013

Keywords:
Universality
DNA
Colorimetry
Graphene oxide
Peroxidase-like activity
Self-assembly

ABSTRACT

We have demonstrated a robust sensing strategy by employing single-stranded probe DNA and the hemin-graphene hybrid (GH) to detect a broad range of targets including metal ions, DNA and small molecules. This nearly "universal" biosensor approach is based on the DNA-mediated assembly of the hemin-graphene composite upon addition of the targets. Afterwards, GH aggregate resulting from DNA hybridization will occur. The DNA-GH hybrids will settle on the bottom of the vial after centrifugation, leaving behind a transparent supernatant. After incubation with TMB and H_2O_2, the colorimetric signal of the centrifugal supernatant will be significantly lower compared to that in the absence of targets. Therefore, mediation of the assembly of DNA on GH by targets can yield a facile means with tunable optical properties in response to concentration changes of the targets. This colorimetric "readout" offers great advantages such as the simple operation process, low-cost portable instrument and easy-to-use applications. Therefore, we believe that this method promises a great potential of becoming a routine tool for quantitative detection of a wide spectrum of analytes for specific applications in biodiagnostics, nanoelectronics, and bionanotechnology.

1. Introduction

The development of universal sensors that can detect a broad range of different targets is highly desirable [1,2], as such versatile platforms with which many analyses can be performed in a single system are attractive from an economic point of view. However, until now, very few universal detection systems have been developed [3–5], which may greatly limit the development of the sensing technology. Therefore, the search for universal systems with high specificity and sensitivity still remains a big challenge.

Recently, the emergence of a new generation of hybrid nanomaterials offers great opportunities in the field of sensing and drug delivery [6]. Especially, graphene and its water-soluble derivative, graphene oxide (GO), have attracted great interest for these applications [7–10]. The unique capacity of graphene or graphene oxide (GO) in adsorbing biomolecules, such as nucleic acids and proteins, with super fluorescence quenching efficiency creates a robust platform for the development of fluorescent biosensors [11–18]. Although the existing fluorescence methods have their own advantages, most of them still require tedious fluorophore labeling processes and time-consuming purification steps [19]. To circumvent the limitations pertinent to fluorescence detection, it is imperative to exploit alternative methods for quantitative detection in a simpler and more straightforward manner [20].

The inherent superiorities of colorimetry, such as simplicity, low cost, and label-freeness, make it very attractive for target detection. Lately, efforts toward the construction of colorimetric biosensors have been realized by using functionalized graphene derivatives with their intrinsic peroxidase-like activity [21–28]. For example, we recently reported a colorimetric assay for selective, quantitative and fast detection of cancer cells based on the peroxidase-like activity of the hemin-graphene hybrid (GH) [28]. However, until now, a universal biosensing platform based on GH for colorimetric assay has not been reported yet, even though it is urgently required. In light of the above considerations, we sought to develop a robust sensing platform for label-free colorimetric detection of a broad range of targets by utilizing the DNA-mediated assembly of GH.

2. Materials and methods

2.1. Materials and measurements

Graphite was purchased from Sinopharm Chemical Reagent Co. (Shanghai, China). DNA oligonucleotides were obtained from Sangon (Shanghai, China). All other reagents were all of analytical reagent grade and used as received.

* Corresponding authors. Tel./fax: +86 431 85262625.
E-mail addresses: jren@ciac.jl.cn (J. Ren), xqu@ciac.jl.cn (X. Qu).

0142-9612/$ – see front matter © 2013 Elsevier Ltd. All rights reserved.
http://dx.doi.org/10.1016/j.biomaterials.2013.03.039

Kinetic measurements were carried out in time course mode by monitoring the absorbance change at 652 nm on a Jasco-V550 UV–Vis spectrophotometer. AFM measurements were performed by using a Nanoscope V multimode atomic force microscope (Veeco Instruments, USA). Dynamic light scattering (DLS) measurements were performed on a WyattQELS instrument with a vertically polarized He–Ne laser (DAWN EOS, Wyatt Technology). The scattering angle was fixed at 90°.

2.2. Synthesis of graphene oxide (GO)

GO was synthesized from graphite powder based on the Hummer's method [31]. Pretreated graphite powder was put into 0 °C concentrated H_2SO_4 (120 mL). Then, $KMnO_4$ (15 g) was added gradually under stirring, and the temperature of the mixture was kept below 20 °C by an ice bath. Successively, the mixture was stirred at 35 °C for 4 h and then diluted with deionized water (250 mL) by keeping the temperature under 50 °C. Water (700 mL) was then injected into the mixture followed by adding H_2O_2 (30 wt%) (20 mL) drop by drop. The mixture was filtered and washed with aqueous HCl solution (v/v 1:10) (1 L) to remove metal ions followed by deionized water to remove the acid. The resulting solid was dried in air and diluted to make a GO dispersion (0.5 wt%). Finally, it was purified by dialysis for 1 week to remove the remaining metal species. Exfoliation was carried out by sonicating the GO dispersion (0.1 mg/mL) under ambient conditions for 1 h.

2.3. Synthesis of hemin functionalized graphene nanosheets (GH)

GH were prepared according to a previously reported method [21]. Generally, GH were synthesized by a simple strategy through the π–π stacking interactions. 20.0 mL of the homogenous graphene oxide dispersion (0.5 mg/mL) was mixed with 20.0 mL of 0.5 mg/mL hemin aqueous solution and 200 μL of ammonia solution, followed by the addition of 30 μL of hydrazine solution. After being vigorously shaken or stirred for a few minutes, the vial was put in a water bath (60 °C) for 3.5 h. The stable black dispersion was obtained.

2.4. Synthesis of DNA-GH conjugates

In a typical procedure, GH aqueous solution (500 μL, 0.2 mg/mL) and DNA (4 μM) were mixed in aqueous Tris–EDTA buffer (10 mM Tris–HCl, 10 mM EDTA, pH 8.0) by sonicating for 10 min and then incubated at room temperature for 24 h, and the concentration of NaCl was slowly increased to 10 mM during the incubation. To remove free hemin and unbound DNA, the solution was centrifuged at 13,000 rpm for 30 min, the supernatant was discarded, and the precipitated DNA-GH conjugates were then redispersed in Tris–EDTA buffer. This precipitation-redispersion process could be repeated several times to guarantee a complete removal of free hemin and unbound DNA.

2.5. Target detection

DNA-GH conjugates (100 μL) were mixed together and the target (10 μL) solutions with different concentrations were then added respectively. The mixture remained in Tris–EDTA buffer for 12 h at room temperature. All the samples were centrifuged at 5000 rpm for 15 min, and the supernatants were collected. In a typical test, chemicals were added into 460 μL buffer solution (25 mM Na_2HPO_4, pH 4.0) in an order of 10 μL supernatants mentioned above, 8 μL TMB (final concentration 800 μM), and 25 μL H_2O_2 (final concentration 50 mM). Kinetic measurements were carried out in time course mode by monitoring the absorbance change at 652 nm on a Jasco-V550 UV–Vis spectrophotometer.

3. Results and discussion

The working principle of our work is schematically represented in Scheme 1. Initially, the hemin–graphene hybrid nanosheets (GH) are synthesized according to the previously established method [28]. The as-prepared GH have the intrinsic peroxidase-like activity, which can catalyze the reaction of peroxidase substrate 3,3′,5,5′-tetramethylbenzidine (TMB) in the presence of H_2O_2. Then the DNA probes are separately added to GH solutions to form the DNA-GH hybrids. Every DNA probe has a target-specific sequence and a tail to facilitate the assembly of DNA probe on GH nanosheets. In the absence of the target, the DNA-GH hybrids can be stably suspended in the solution after centrifugation. When the above solution is incubated with TMB and H_2O_2, the GH centrifugal supernatant will catalyze a color reaction that can be judged by the naked eye and easily be monitored by the absorbance changes at 652 nm. However, upon addition of the target, GH aggregate resulting from DNA hybridization will occur [29]. Then, the DNA-GH hybrids will settle on the bottom of the vials after centrifugation, leaving behind a transparent supernatant. As a result, the absorbance signal of the centrifugal supernatant is significantly lower. Mediation of the assembly of DNA on GH by targets can yield a facile means with tunable optical properties in response to concentration changes of the targets. Therefore, the DNA-controlled assembly of GH can be successfully applied for label-free colorimetric detection of a panel of targets. Furthermore, this colorimetric "readout" offers additional advantages such as the simple

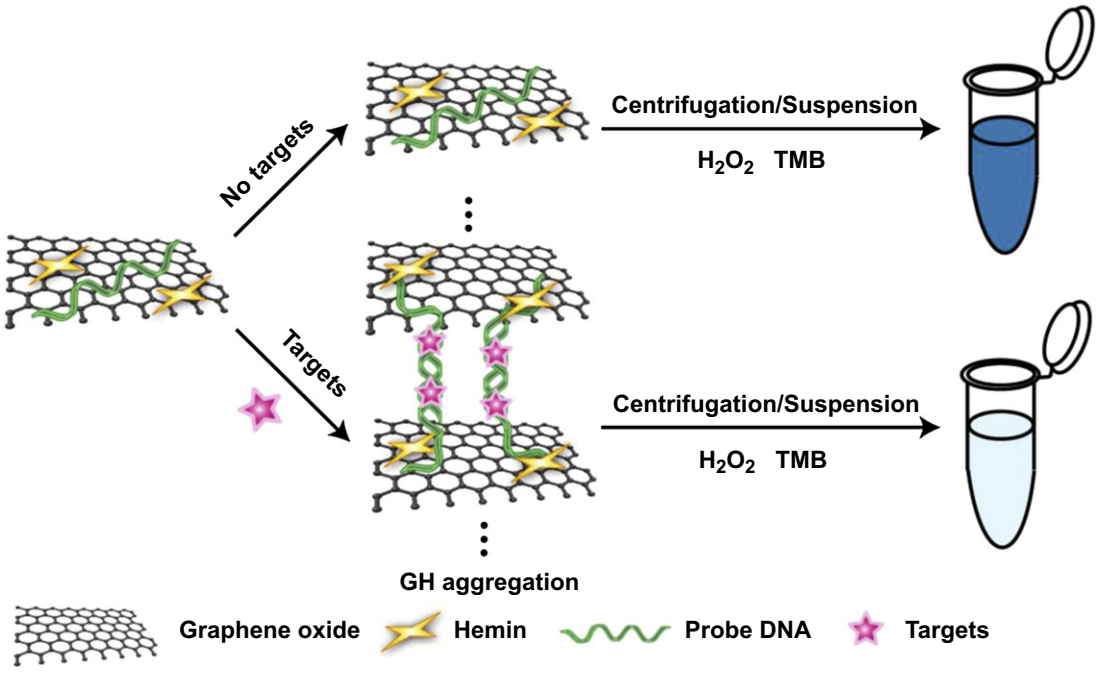

Scheme 1. Schematic illustration of procedures for targets detection.

operation process, low-cost portable instrument and easy-to-use applications [30].

3.1. Sensor fabrication

In the biosensing system, GO was prepared according to a modified Hummers method from graphite powders [31]. The typical morphology of GO was shown in atomic force microscopy (AFM) image (Figure S1a), indicating that the thickness of the graphene layer was around 1.2 nm (Figure S1c) [32,33]. Next, the attachment of hemin on graphene surface (GH) was also characterized by AFM (Figure S1b) and UV–Vis absorption spectroscopy (Figure S2). AFM study showed that the thickness of GH was determined to be about 1.7 nm (Figure S1d), with an increment of 0.5 nm compared with that of unmodified graphene, owing to the presence of hemin on the graphene sheet surfaces [21]. In addition, an absorption at 418 nm was also observed after reduction (Figure S2), which further clarified that hemin molecules were attached to graphene [21,34].

3.2. Detection of Hg^{2+} ions

To examine the ability of our GH-based assay to detect metal ions, we chose Hg^{2+} as a model molecule. Mercury was one of the most potent toxicants in the world. The exposure to mercury even at very low concentration would result in digestive, kidney and especially neurological diseases [35,36]. Therefore, the probe of Hg^{2+} ions was a focus of many research endeavors. The design of the GH-based sensor for Hg^{2+} ions detection was shown in Fig. 1a. Firstly, DNA1-GH and DNA2-GH hybrids were prepared by incubation of the as-prepared GH with ssDNA (DNA1 or DNA2) and then ultracentrifuged to remove free DNA. Both of the DNA1 and DNA2

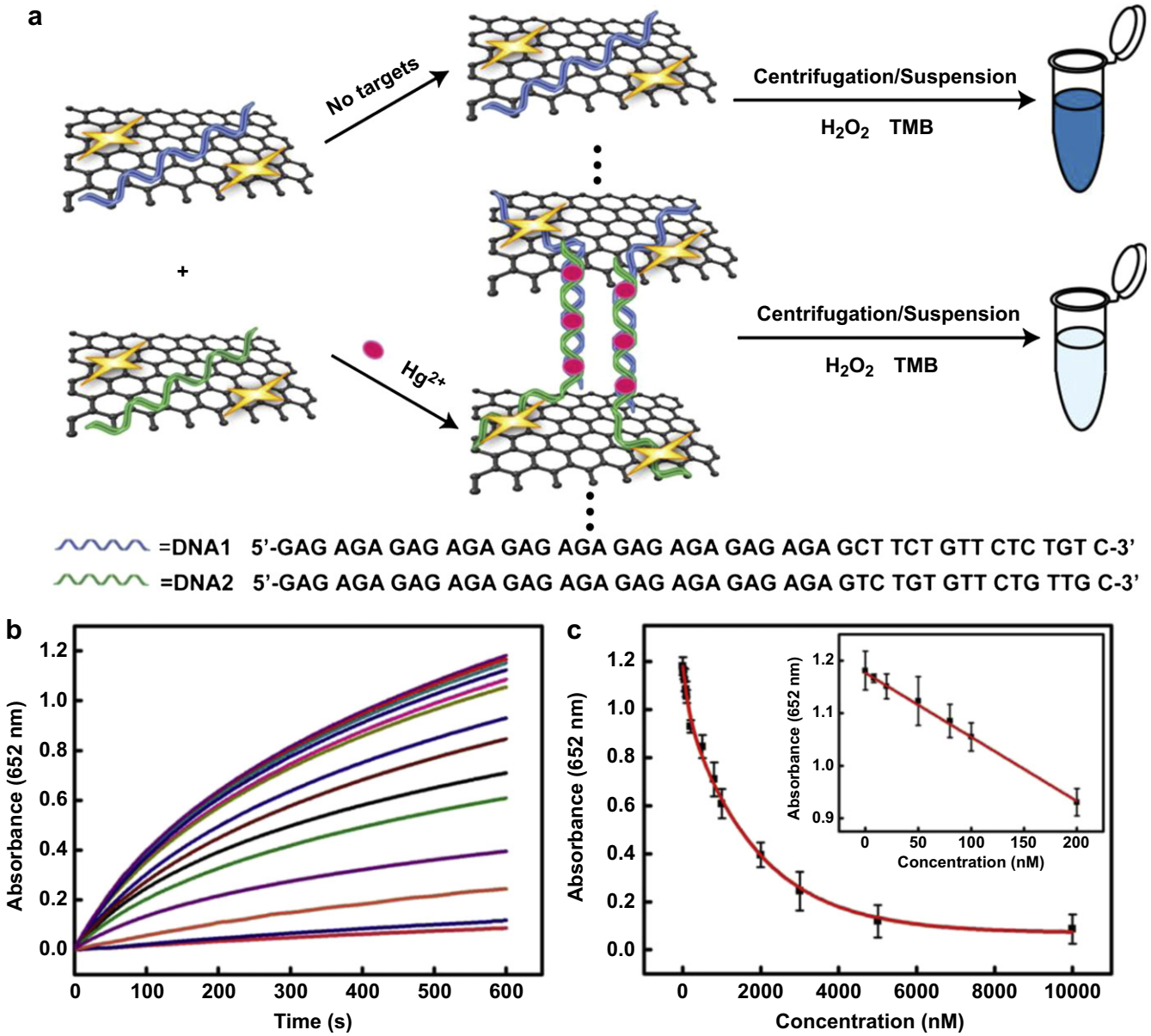

Fig. 1. a) Schematic illustration of procedures for Hg^{2+} ions detection. b) Time-dependent absorbance changes at 652 nm in the presence of different amounts of Hg^{2+} ions ranging from 0 to 10,000 nM (0, 8, 20, 50, 80, 100, 200, 500, 800, 1000, 2000, 3000, 5000, 10,000 nM). c) Calibration curve corresponding to the absorbance for various concentrations of Hg^{2+} ions after an interval of 10 min. Inset: the linear plot. The error bars represent the standard deviation of three measurements.

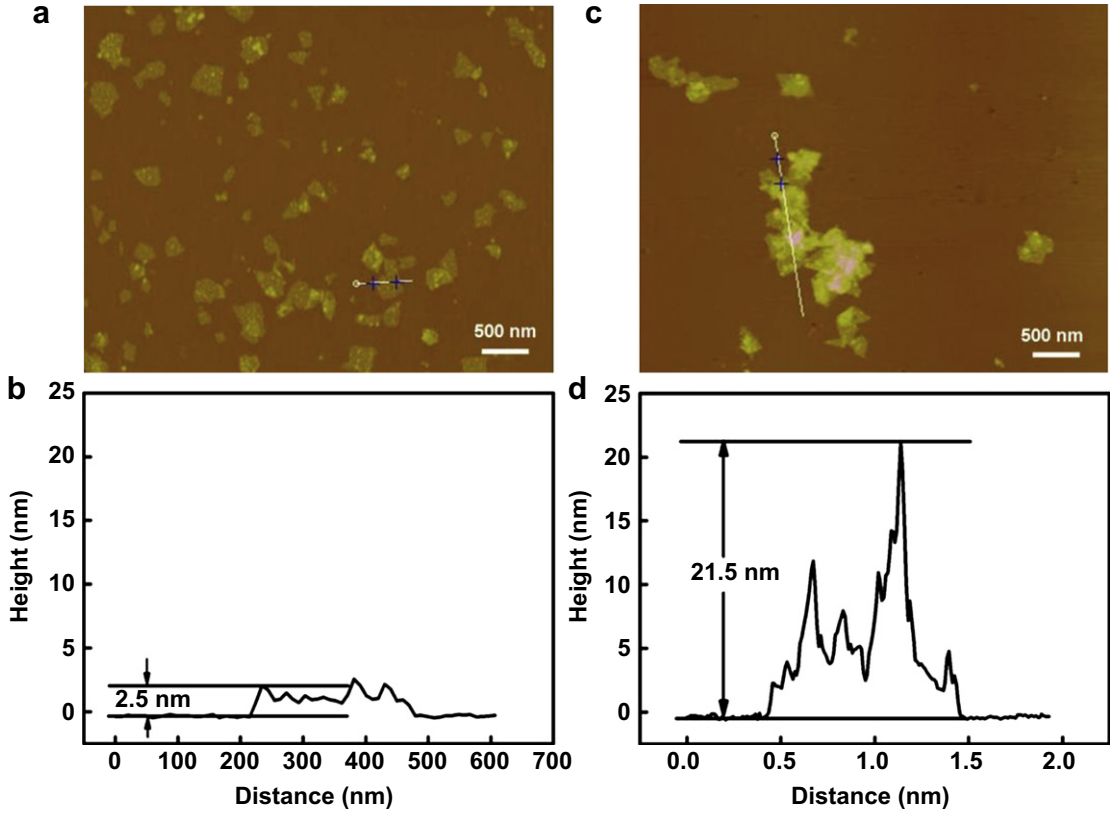

Fig. 2. AFM images and height profiles of DNA-GH complex (a, b) and DNA-GH aggregate (c, d) formed from DNA1-GH and DNA2-GH mixing hybrids with 5 μM Hg^{2+} ions.

sequences had a T-rich sequence and a $d(GA)_{15}$ tail to facilitate the assembly of DNA on GH nanosheets. These two T-rich sequences were complementary except for the deliberately designed T–T mismatches. In the absence of Hg^{2+} ions, DNA1 and DNA2 were not capable of hybridization. Therefore, the DNA1-GH and DNA2-GH hybrids could remain suspended in aqueous solution efficiently after centrifugation. These samples exhibited a high absorbance signal. However, when Hg^{2+} ions were present, DNA hybridization would occur due to the formation of thymine–Hg^{2+}–thymine (T–Hg^{2+}–T) base pairs [37]. As a result, large aggregates could be obtained due to the controllable assembly of the DNA on GH, and the signal of the centrifugal supernatant was largely decreased, as compared to that without Hg^{2+} ions.

AFM was used to visualize the typical morphology of DNA-GH hybrids and the aggregates. Fig. 2a showed the typical AFM image of the DNA-GH hybrids, where the white areas on the GO surfaces might be due to the presence of DNA [32]. Upon mixing the DNA-GH hybrids with 5 μM Hg^{2+} ions, large aggregates could be obtained due to the occurrence of hybridization of DNA1 and DNA2 with the formation of T–Hg^{2+}–T pairs, as observed in AFM investigation (Fig. 2c). The height of section extracted from the typical AFM image indicated that the DNA-mediated GH aggregate was 5–21.5 nm in apparent thickness (Fig. 2d). It was obvious that such aggregate height data were consistent with the thickness of multilayers of DNA functional GH nanosheets. In addition, the DNA-GH hybrids before and after addition of Hg^{2+} ions were also directly measured by dynamic light scattering (DLS) technique, making it feasible to determine actual sizes of the DNA-GH hybrid samples in aqueous solution. As shown in Figure S3, the hydrodynamic diameter of DNA-GH hybrids increased from 175 to 840 nm upon the addition of 5 μM Hg^{2+} ions, indicating the large aggregates of GH [29]. All these results demonstrated that the DNA-GH hybrids could serve as a good candidate for quantitative detection of Hg^{2+} ions.

To evaluate the sensitivity of the assay, the sensor solutions were treated with Hg^{2+} ions of various concentrations, and the absorption spectra were measured. Fig. 1b showed the time-dependent absorbance changes in the presence of different amounts of Hg^{2+} ions. The absorbance changes were retarded as the concentration of Hg^{2+} ions increased, which was attributed to

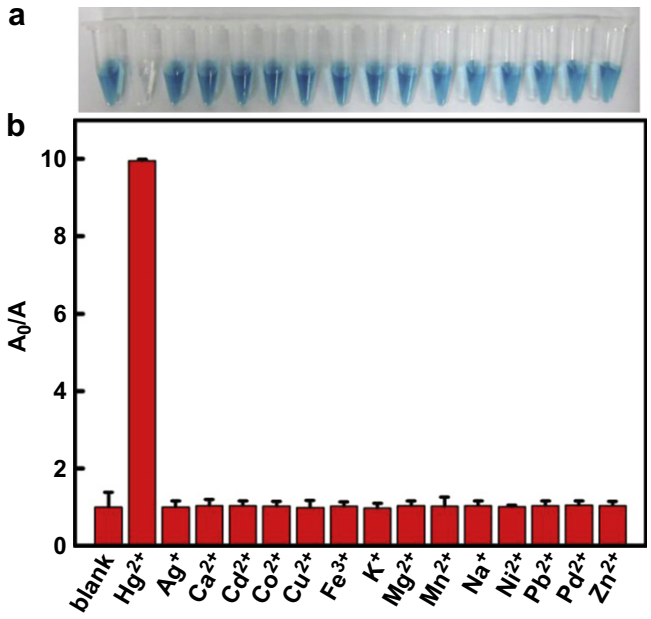

Fig. 3. Selectivity analysis for Hg^{2+} ions detection by monitoring the color changes a) and the relative absorbances b). The concentration of each metal ion is 5 μM. The error bars represent the standard deviation of three measurements.

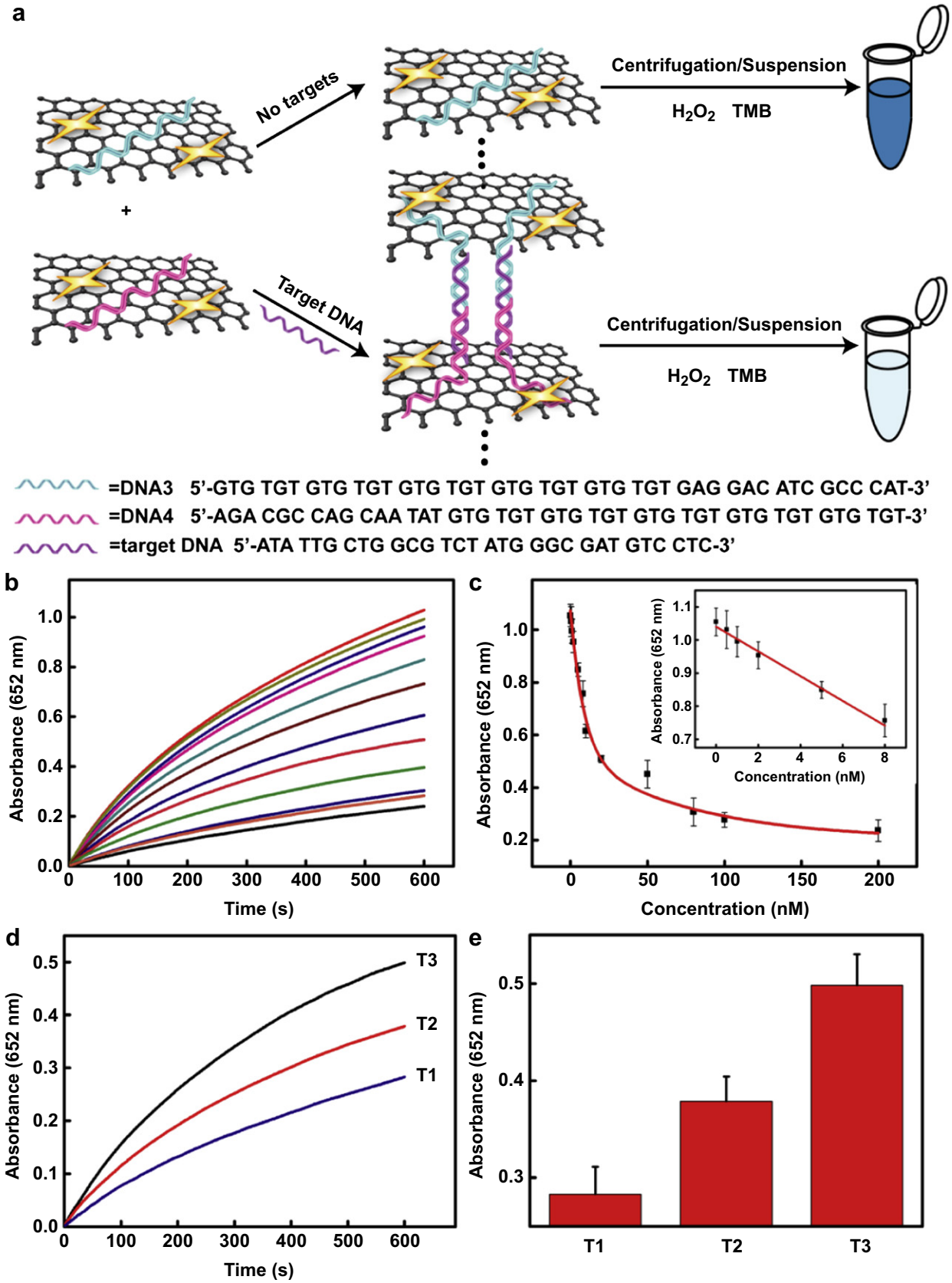

Fig. 4. a) Schematic illustration of procedures for DNA detection. b) Time-dependent absorbance changes at 652 nm in the presence of different amounts of DNA ranging from 0 to 200 nM (0, 0.5, 1, 2, 5, 8, 10, 20, 50, 80, 100, 200 nM). c) Calibration curve corresponding to the absorbance for various concentrations of DNA after an interval of 10 min. Inset: the linear plot. d) Time-dependent absorbance at 652 nm with corresponding supernatant solution of the DNA-GH hybrids with 100 nM T1; 100 nM T2 and 100 nM T3. e) The corresponding absorbance histograms. Error bars indicated the relative standard deviation of three repeated experiments.

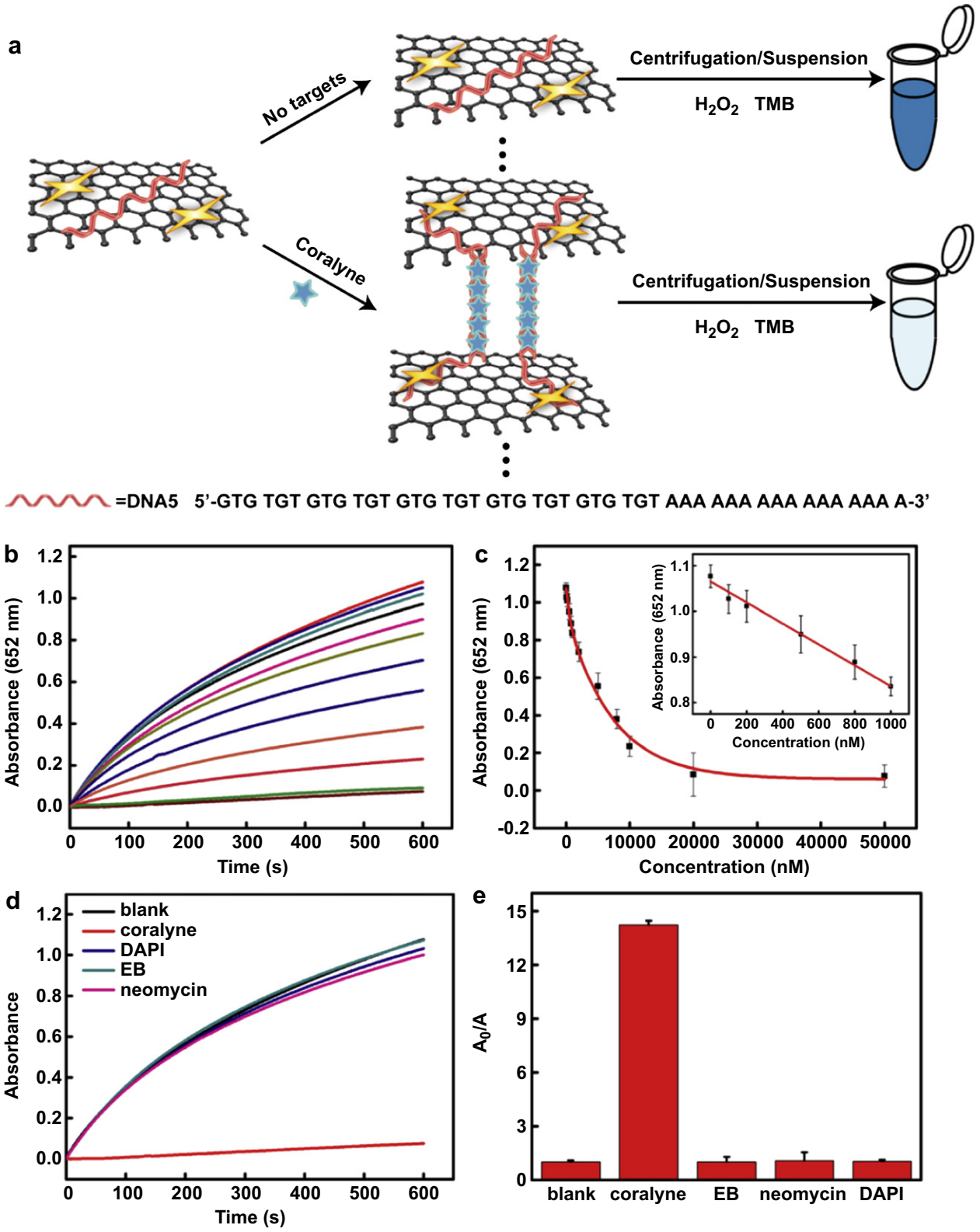

Fig. 5. a) Schematic illustration of procedures for coralyne detection. b) Time-dependent absorbance changes at 652 nm in the presence of different amounts of coralyne ranging from 0 to 50 μM (0, 100, 200, 500, 800, 1000, 2000, 5000, 8000, 10,000, 20,000, 50,000 nM). c) Calibration curve corresponding to the absorbance for various concentrations of coralyne after an interval of 10 min. Inset: the linear plot. d) Time-dependent absorbance changes at 652 nm in the absence and presence of different binders (20 μM). e) The absorbance ratio A_0/A in the presence of 20 μM coralyne or other small molecules (where A_0 and A are the absorbance of TMB in the absence and presence, respectively, of the small molecules). Error bars indicated the relative standard deviation of three repeated experiments.

the aggregation of GH. The absorption changes from before Hg^{2+} ions binding to after Hg^{2+} ions binding directly reflected how much Hg^{2+} ions were present in the solution (Fig. 1c). A linear relationship was observed in the concentration range from 8 nM to 200 nM, where Hg^{2+} ions were able to be quantitatively measured. The detection limit in our work was estimated to be 8 nM, which was lower than the Hg^{2+} detection requirement for drinking water of U.S. Environmental Protection Agency with the maximum contamination level at 10 nM. These data revealed that the DNA-GH hybrids could provide an efficient platform for ultrahigh sensitivity and good linearity for the quantitative analysis of Hg^{2+} ions. To address the specificity of the DNA-GH hybrids, the selectivity of Hg^{2+} ions over the other metal ions was also monitored. As shown in Fig. 3, it was clear that only the solution containing Hg^{2+} ions was colorless and exhibited significantly higher absorption ratio (A_0/A). Whereas solutions containing other interferences all exhibited a deep blue color. Moreover, there was nearly negligible absorbance change in the presence of other metal ions. These results suggested that the specificity of our method was high enough to discriminate between Hg^{2+} ions and the other metal ions.

3.3. Detection of DNA

After observing that GH-based colorimetric assay was effective for Hg^{2+} ions detection, we attempted to use it in the detection of DNA as a first example of the broader applicability of our approach. As we know, sensitive and selective detection of nucleic acids had found widespread applications in gene expression profiling, clinical disease diagnostics, and drug industry [38,39]. Thus, the methods for highly sensitive and selective detection of DNA were an urgent and unmet need. The working principle of our assay for DNA detection was schematically represented in Fig. 4a. Probe DNA3 and DNA4 were separately added to GH solutions to form DNA3-GH and DNA4-GH hybrids, respectively. DNA3 had a target-specific sequence complementary to target DNA (T-DNA) and a $d(GT)_{15}$ tail at the 5′ terminus to facilitate the assembly of DNA3 on GH nanosheets. DNA4 also had a complementary sequence to target T-DNA with a $d(GT)_{15}$ tail at the 3′ terminus. In the mixture of the two DNA3-GH and DNA4-GH hybrids, T-DNA would hybridize with both DNA3 and DNA4, which resulted in an assembly of the GH nanosheets. Therefore, large aggregates could be obtained (Figure S4, S5).

Next, we investigated the concentration dependence of the GH-based assay with the target DNA. Fig. 4b showed time-dependent absorbance changes in the presence of different amounts of target DNA. It was found that the absorbance of the centrifugal supernatants decreased linearly with the concentration of complementary target DNA in the range of 0.5 nM–8 nM with a limit of detection around 0.5 nM (Fig. 4c), comparable to previously reported systems based on MWNT light scattering [40], SWNT near-infrared fluorescence [41], SWNT intrinsic peroxidase activity [42], or GO fluorescence quenching [43]. More importantly, this DNA sensor was of sufficient selectivity to easily differentiate single mismatches, which offered the opportunity to determinate single nucleotide polymorphisms (SNPs). Fig. 4d showed time-dependent absorbance changes obtained by using the DNA-GH hybrids probe toward complementary target T1, one-base mismatched target T2 and two-base mismatched target T3. As can be seen in Fig. 4e, the absorbance change obtained upon addition of 100 nM T2, T3 was about 33.8%, 76.2%, respectively, higher than that for perfect target T1 at the same concentration. This high specificity seemed to be attributed to the synergic and multivalent effects of the DNA-GH hybrids in hybridization with target DNA, in which a single-base mismatch led to synchronous decrease of affinity at all binding sites between the probe DNA and the target DNA [29,44]. This result demonstrated that the single-base-mismatched DNA strands could be directly discriminated from the perfectly complementary targets, indicating the high specificity of this assay.

3.4. Detection of coralyne

To complete the demonstration that our assay was universally applicable to all of the major analyte classes, we investigated whether it could detect small molecules, with coralyne as a model system. Coralyne, a small crescent-shape molecule, was recently shown to be able to bind strongly to single-stranded homo-adenine-containing nucleic acids [45–49]. The presence of coralyne promoted a stable anti-parallel duplex of poly-deoxyadenosine [50]. The design of our strategy for coralyne detecting was shown in Fig. 5a. Firstly, the probe DNA5 could be stably adsorbed on the GH sheets to form the DNA-GH hybrids due to the π-stacking interaction between the ring of nucleobases and the hexagonal cells of the graphene. The DNA5 sequence had an A-rich sequence dA_{16} and a $d(GT)_{15}$ tail at the 5′ terminus to facilitate the assembly of DNA on GH nanosheets. This sequence lacked any secondary structure and resulted in a well-dispersed GO solution (Figure S6a, S7). However, a small molecule such as coralyne should bind strongly, triggering the formation of non-Watson–Crick homo-adenine duplexes, and subsequently could also induce GH aggregation (Figure S6c, S7). As a result, the reduction of the absorption signal intensity of the centrifugal supernatant could be obtained. As shown in Fig. 5b, upon increasing additions of coralyne, as expected, the signal intensity was gradually reduced, which was attributed to the generation of non-Watson–Crick homo-adenine duplex DNA. The relationship between the absorbance at 652 nm and the coralyne concentration was constructed in Fig. 5c. A linear relationship was observed in the concentration range from 0.1 μM to 1 μM. The observed detection limit of coralyne was estimated to be 0.1 μM, which compared well with values obtained from colorimetric analytical techniques based on gold or silver nanoparticles [51]. In order to assess the specificity of the biosensor for coralyne, we chose three typical DNA binders as controls: ethidium bromide (EB; a typical intercalator), 4′, 6-diamidino-2phenylindole (DAPI; a typical minor grove binder), and neomycin (a typical major grove binder). As shown in Fig. 5d, EB, DAPI, and neomycin (20 μM) caused no noticeable changes in absorption signals, while the absorption signal was greatly decreased by the addition of coralyne (20 μM), demonstrating that the biosensor had a highly selective response to coralyne. In addition, by employing the binding-induced folding or association of aptamers, we reasoned that our strategy could be adopted for the detection of other analytes.

4. Conclusion

In summary, by adapting a series of DNA probes, we take advantage of DNA-controlled assembly of GH to create a sensitive colorimetric label-free assay for diverse targets detection including metal ions, DNA and small molecules. This method relies on the optical absorbance signals decrease that occurs as a result of DNA-mediated GH aggregate upon addition of the targets. No sophisticated experimental techniques or chemical modifications for DNA are required. In addition, the use of the target-specific probe DNA imparts extraordinarily high selectivity to the sensor, and the application of the colorimetric method also brings ultrahigh sensitivity. Considering the superior sensitivity and specificity, as well as the multiplex and simple-to-implement features, this method promises a great potential of becoming a routine tool for quantitative detection of a wide spectrum of analytes for specific applications in biodiagnostics, nanoelectronics, and bionanotechnology.

Acknowledgments

The authors are grateful for the referee's helpful comments on the manuscript. Financial support was provided by the National Basic Research Program of China (2011CB936004 and 2012CB720602) and the National Natural Science Foundation of China (Grants 91213002, 21210002, 21072182).

Appendix A. Supplementary data

Supplementary data related to this article can be found at http://dx.doi.org/10.1016/j.biomaterials.2013.03.039.

References

[1] Das J, Cederquist KB, Zaragoza AA, Lee PE, Sargent EH, Kelley SO. An ultrasensitive universal detector based on neutralizer displacement. Nat Chem 2012;4:642–8.
[2] Liu Y, Ren J, Qin Y, Li J, Liu J, Wang E. An aptamer-based keypad lock system. Chem Commun 2012;48:802–4.
[3] Zheng D, Zou R, Lou X. Label-free fluorescent detection of ions, proteins, and small molecules using structure-switching aptamers, SYBR gold, and exonuclease I. Anal Chem 2012;84:3554–60.
[4] Zhang M, Yin BC, Tan W, Ye BC. A versatile graphene-based fluorescence "on/off" switch for multiplex detection of various targets. Biosens Bioelectron 2011;26:3260–5.
[5] Xia F, Zuo XL, Yang RQ, Xiao Y, Kang D, Vallee-Belisle A, et al. Colorimetric detection of DNA, small molecules, proteins, and ions using unmodified gold nanoparticles and conjugated polyelectrolytes. Proc Natl Acad Sci U S A 2010;107:10837–41.
[6] Giljohann DA, Seferos DS, Daniel WL, Massich MD, Patel PC, Mirkin CA. Gold nanoparticles for biology and medicine. Angew Chem Int Ed 2010;49:3280–94.
[7] Dreyer DR, Ruoff RS, Bielawski CW. From conception to realization: an historial account of graphene and some perspectives for its future. Angew Chem Int Ed 2010;49:9336–44.
[8] Feng L, Chen Y, Ren J, Qu X. A graphene functionalized electrochemical aptasensor for selective label-free detection of cancer cells. Biomaterials 2011;32:2930–7.
[9] Guo S, Dong S. Graphene nanosheet: synthesis, molecular engineering, thin film, hybrids, and energy and analytical applications. Chem Soc Rev 2011;40:2644–72.
[10] Yang X, Zhang X, Ma Y, Huang Y, Wang Y, Chen Y. Superparamagnetic graphene oxide-Fe_3O_4 nanoparticles hybrid for controlled targeted drug carriers. J Mater Chem 2009;19:2710–4.
[11] Hu Y, Wang K, Zhang Q, Li F, Wu T, Niu L. Decorated graphene sheets for label-free DNA impedance biosensing. Biomaterials 2011;33:1097–106.
[12] Wu S, Duan N, Ma X, Xia Y, Wang H, Wang Z, et al. Multiplexed fluorescence resonance energy transfer aptasensor between upconversion nanoparticles and graphene oxide for the simultaneous determination of mycotoxins. Anal Chem 2012;84:6263–70.
[13] Zhang C, Yuan Y, Zhang S, Wang Y, Liu Z. Biosensing platform based on fluorescence resonance energy transfer from upconverting nanocrystals to graphene oxide. Angew Chem Int Ed 2011;50:6851–4.
[14] Xing XJ, Liu XG, Yue H, Luo QY, Tang HW, Pang DW. Graphene oxide based fluorescent aptasensor for adenosine deaminase detection using adenosine as the substrate. Biosens Bioelectron 2012;37:61–7.
[15] Pei H, Li J, Lv M, Wang J, Gao J, Lu J, et al. A graphene-based sensor array for high-precision and adaptive target identification with ensemble aptamers. J Am Chem Soc 2012;134:13843–9.
[16] Wang L, Pu KY, Li J, Qi X, Li H, Zhang H, et al. A graphene–conjugated oligomer hybrid probe for light-up sensing of lectin and Escherichia coli. Adv Mater 2011;23:4386–91.
[17] Wang H, Zhang Q, Chu X, Chen T, Ge J, Yu R. Graphene oxide–peptide conjugate as an intracellular protease sensor for caspase-3 activation imaging in live cells. Angew Chem Int Ed 2011;31:7065–9.
[18] Hu Y, Li F, Bai X, Li D, Hua S, Wang K, et al. Label-free electrochemical impedance sensing of DNA hybridization based on functionalized graphene sheets. Chem Commun 2011;47:1743–5.
[19] Ohno Y, Maehashi K, Yamashiro Y, Matsumoto K. Electrolyte-gated graphene field-effect transistors for detecting pH and protein adsorption. Nano Lett 2009;9:3318–22.
[20] Shen W, Deng H, Gao Z. Gold nanoparticle-enabled real-time ligation chain reaction for ultrasensitive detection of DNA. J Am Chem Soc 2012;134:14678–81.
[21] Guo Y, Deng L, Li J, Guo S, Wang E, Dong S. Hemin–graphene hybrid nanosheets with intrinsic peroxidase-like activity for label-free colorimetric detection of single-nucleotide polymorphism. Acs Nano 2011;5:1282–90.
[22] Liu M, Zhao H, Chen S, Yu H, Quan X. Interface engineering catalytic graphene for smart colorimetric biosensing. Acs Nano 2012;6:3142–51.
[23] Song YJ, Qu KG, Zhao C, Ren JS, Qu XG. Graphene oxide: intrinsic peroxidase catalytic activity and its application to glucose detection. Adv Mater 2010;22:2206.
[24] Xue T, Jiang S, Qu Y, Su Q, Cheng R, Dubin S, et al. Graphene-supported hemin as a highly active biomimetic oxidation catalyst. Angew Chem Int Ed 2012;51:3822–5.
[25] Liu M, zhao h, Chen S, Yu H, Quan X. Stimuli-responsive peroxidase mimicking at a smart graphene interface. Chem Commun 2012;48:7055–7.
[26] Chen H, Li Y, Zhang F, Zhang G, Fan X. Graphene supported Au-Pd bimetallic nanoparticles with core-shell structures and superior peroxidase-like activities. J Mater Chem 2011;21:17658–61.
[27] Dong YL, Zhang HG, Rahman ZU, Su L, Chen XJ, Hu J, et al. Graphene oxide-Fe_3O_4 magnetic nanocomposites with peroxidase-like activity for colorimetric detection of glucose. Nanoscale 2012;4:3969–76.
[28] Song Y, Chen Y, Feng L, Ren J, Qu X. Selective and quantitative cancer cell detection using target-directed functionalized graphene and its synergetic peroxidase-like activity. Chem Commun 2011;47:4436–8.
[29] Tang L, Wang Y, Liu Y, Li J. DNA-directed self-assembly of graphene oxide with applications to ultrasensitive oligonucleotide assay. Acs Nano 2011;5:3817–22.
[30] Chen L. Ultrasensitive colorimetric detection of heparin based on self-assembly of gold nanoparticles on graphene oxide. Analyst 2012;137:3653–8.
[31] Hummers WS, Offeman RE. Preparation of graphitic oxide. J Am Chem Soc 1958;80:1339.
[32] Lu CH, Yang HH, Zhu CL, Chen X, Chen GN. A graphene platform for sensing biomolecules. Angew Chem Int Ed 2009;48:4785–7.
[33] Lu CH, Li J, Liu JJ, Yang HH, Chen X, Chen GN. Increasing the sensitivity and single-base mismatch selectivity of the molecular beacon using graphene oxide as the "nanoquencher". Chem-Eur J 2010;16:4889–94.
[34] Xu Y, Zhao L, Bai H, Hong W, Li C, Shi G. Chemically converted graphene induced molecular flattening of 5,10,15,20-tetrakis(1-methyl-4-pyridinio) porphyrin and its application for optical detection of cadmium(II) ions. J Am Chem Soc 2009;131:13490–7.
[35] Clarkson TW, Magos L, Myers GJ. The toxicology of mercury-current exposures and clinical manifestations. N Engl J Med 2003;349:1731–7.
[36] Clarkson TW, Magos L, Myers GJ. Human exposure to mercury: the three modern dilemmas. J Trace Elem Exp Med 2003;16:321–43.
[37] Freeman R, Finder T, Willner I. Multiplexed analysis of Hg^{2+} and Ag^{+} ions by nucleic acid functionalized CdSe/ZnS quantum dots and their use for logic gate operations. Angew Chem Int Ed 2009;48:7818–21.
[38] Tyagi S, Bratu DP, Kramer FR. Multicolor molecular beacons for allele discrimination. Nat Biotechnol 1998;16:49–53.
[39] Heller MJ. DNA microarray technology: devices, systems, and applications. Annu Rev Biomed Eng 2002;4:129–53.
[40] Zhang L, Huang CZ, Li YF, Xiao SJ, Xie JP. Label-free detection of sequence-specific DNA with multiwalled carbon nanotubes and their light scattering signals. J Phys Chem B 2008;112:7120–2.
[41] Jeng ES, Moll AE, Roy AC, Gastala JB, Strano MS. Detection of DNA hybridization using the near-infrared band-gap fluorescence of single-walled carbon nanotubes. Nano Lett 2006;6:371–5.
[42] Song YJ, Wang XH, Zhao C, Qu KG, Ren JS, Qu XG. Label-free colorimetric detection of single nucleotide polymorphism by using single-walled carbon nanotube intrinsic peroxidase-like activity. Chem-Eur J 2010;16:3617–21.
[43] He S, Song B, Li D, Zhu C, Qi W, Wen Y, et al. A graphene nanoprobe for rapid, sensitive, and multicolor fluorescent DNA analysis. Adv Funct Mater 2010;20:453–9.
[44] Tang Z, Wu H, Cort JR, Buchko GW, Zhang Y, Shao Y, et al. Constraint of DNA on functionalized graphene improves its biostability and specificity. Small 2010;6:1205–9.
[45] Lin YH, Tseng WL. Fluorescence detection of coralyne and polyadenylation reaction using an oligonucleotide-based fluorogenic probe. Chem Commun 2011;47:11134–6.
[46] Song GT, Chen C, Qu XG, Miyoshi D, Ren JS, Sugimoto N. Small-molecule-directed assembly: a gold nanoparticle-based strategy for screening of homoadenine DNA duplex binders. Adv Mater 2008;20:706.
[47] Ren J, Chaires JB. Sequence and structural selectivity of nucleic acid binding ligands. Biochemistry 1999;38:16067–75.
[48] Tseng WL, Lin YH. A room-temperature adenosine-based molecular beacon for highly sensitive detection of nucleic acids. Chem Commun 2012;48:6262–4.
[49] Persil Ö, Santai CT, Jain SS, Hud NV. Assembly of an antiparallel homo-adenine DNA duplex by small-molecule binding. J Am Chem Soc 2004;126:8644–5.
[50] Joung IS, Persil Çetinkol Ö, Hud NV, Cheatham TE. Molecular dynamics simulations and coupled nucleotide substitution experiments indicate the nature of A·A base pairing and a putative structure of the coralyne-induced homoadenine duplex. Nucleic Acids Res 2009;37:7715–27.
[51] Wang Y, Wang J, Yang F, Yang X. Probing biomolecular interactions with dual polarization interferometry: real-time and label-free coralyne detection by use of homoadenine DNA oligonucleotide. Anal Chem 2012;84:924–30.